BIOCHEMISTRY
including biophysical chemistry & molecular biology

Article

pubs.acs.org/biochemistry

Kinetically Competing Huntingtin Aggregation Pathways Control Amyloid Polymorphism and Properties

Murali Jayaraman,[†,‡,§] Rakesh Mishra,[†,‡] Ravindra Kodali,[†,‡] Ashwani K. Thakur,[†,‡,⊥] Leonardus M. I. Koharudin,[†] Angela M. Gronenborn,[†] and Ronald Wetzel*[,†,‡]

[†]Department of Structural Biology and [‡]Pittsburgh Institute for Neurodegenerative Diseases, University of Pittsburgh School of Medicine, Pittsburgh, Pennsylvania 15260, United States

Supporting Information

ABSTRACT: In polyglutamine (polyQ) containing fragments of the Huntington's disease protein huntingtin (htt), the N-terminal 17 amino acid htt^{NT} segment serves as the core of α-helical oligomers whose reversible assembly locally concentrates the polyQ segments, thereby facilitating polyQ amyloid nucleation. A variety of aggregation inhibitors have been described that achieve their effects by neutralizing this concentrating function of the htt^{NT} segment. In this paper we characterize the nature and limits of this inhibition for three means of suppressing htt^{NT}-mediated aggregation. We show that the previously described action of htt^{NT} peptide-based inhibitors is solely due to their ability to suppress the htt^{NT}-mediated aggregation pathway. That is, under htt^{NT} inhibition, nucleation of polyQ amyloid formation by a previously described alternative nucleation mechanism proceeds unabated and transiently dominates the aggregation process. Removal of the bulk of the htt^{NT} segment by proteolysis or mutagenesis also blocks the htt^{NT}-mediated pathway, allowing the alternative nucleation pathway to dominate. In contrast, the previously described immunoglobulin-based inhibitor, the antihtt^{NT} V_L 12.3 protein, effectively blocks both amyloid pathways, leading to stable accumulation of nonamyloid oligomers. These data show that the htt^{NT}-dependent and -independent pathways of amyloid nucleation in polyQ-containing htt fragments are in direct kinetic competition. The results illustrate how amyloid polymorphism depends on assembly mechanism and kinetics and have implications for how the intracellular environment can influence aggregation pathways.

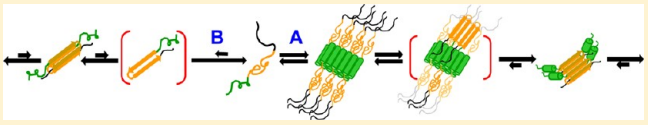

The expanded CAG repeat diseases are a series of familial neurodegenerative conditions resulting from the expansion of a polyglutamine (polyQ) tract in a disease protein.[1] While disease mechanisms remain obscure, the early cellular events are presumably triggered by pathogenic interactions between one or more cellular targets and either monomers or aggregates of the expanded polyQ protein.[2] The polyQ repeat length dependence of both disease risk and disease onset[1] correlates with the repeat length dependence of aggregation onset,[3,4] and polyQ-containing aggregates are found in victims of each of these diseases.[1,5] The detailed structures of the toxic species and the identities of their cellular targets are not known.

As with many other aggregation disease proteins,[6−11] polyQ proteins are able to form a number of polymorphic aggregates both *in vitro* and *in vivo*.[2,12,13] Simple polyQ peptides, flanked by a few charged residues, undergo classical nucleated growth polymerization into amyloid fibrils without the intervention of the kind of nonamyloid oligomeric species often observed in amyloid formation by disease proteins like Aβ.[2,14,15] In contrast, polyQ fused to some flanking sequences, such as the 17 amino acid N-terminus (htt^{NT}) of the Huntington's disease (HD) protein huntingtin (htt), exhibit early formation of roughly spherical oligomers lacking β-structure, and these oligomers play critical roles in the formation of mature polyQ-core amyloid.[2,16−18] Aggregates of a wide range of morphologies have been isolated from a HD tg mouse model,[13] and it is a reasonable possibility that only some of these aggregate polymorphs might be toxic. If so, it becomes particularly important to understand how the cellular environment interacts with the polyQ protein sequence to direct the formation of different aggregate morphologies.

Previous studies uncovered evidence that different growth conditions give rise to aggregates of polyQ-containing htt fragments that exhibit different morphologies and cytotoxicities.[19] More recently, it was demonstrated that aggregates isolated from a number of HD tg mouse models are capable of seeding polyQ aggregation *in vitro*,[20] suggesting an amyloid-like morphology and consistent with toxicity mechanisms postulating recruitment of normal polyQ proteins into aggregates.[21,22] Alternatively, nonamyloid oligomeric forms of htt fragments might be the toxic agents, consistent with the current view of aggregate toxicity in other disease states.[8−10,23] However, there is also some recent indirect evidence against a toxic role for such oligomers, in that analogues of polyQ-containing htt fragments that appear to be only capable of forming nonamyloid oligomers[18] are not toxic when expressed in mammalian cells.[24,25] The open question as to the nature of the toxic species in HD emphasizes the importance of better understanding the htt aggregation pathway and how it might be impacted by interactions with other molecules.

Received: January 20, 2012
Revised: March 5, 2012
Published: March 20, 2012

In this paper we describe how the aggregation reactions and products of polyQ-containing htt fragment model peptides are modified by certain effector molecules and protein modifications relevant to the cellular environment. We find that some events that target the key role of the htt^{NT} segment can delay htt^{NT}-mediated polyQ aggregation, providing a window for the operation of the normally underrepresented aggregation pathway analogous to that for simple polyQ peptides. Another htt^{NT} targeting inhibitor, in contrast, completely blocks nucleation of amyloid by any mechanism, leading to the stable accumulation of large nonamyloid oligomers. The results show that polyQ-containing htt fragments are capable of engaging at least three aggregation pathways leading to different aggregate products and that the relative kinetics of these pathways can be influenced by other molecules and interactions. Since the different pathways generate aggregates of different structures and properties, the possibility exists for modulating toxicity not only by eliminating aggregation but also by its redirection toward more benign aggregated products.

MATERIALS AND METHODS

Materials. Synthetic peptides were obtained in unpurified form from the Keck Biotechnology Center at Yale and were HPLC purified and disaggregated using a combination of aggregate dissociation and ultracentrifugation, as described.[26] In some peptides an F17W mutation is present; previously, we found that this mutation has a negligible effect on aggregation.[16] Acetonitrile, hexafluoroisopropanol (99.5%, spectrophotometric grade), and formic acid were from Acros Organics, and trifluoroacetic acid (99.5%, Sequanal grade) was from Pierce.

General Methods. The sedimentation assay,[26] the ThT and 90° light scattering assays,[27] and the nucleation kinetics analysis[14,26] have been described. The isolation of aggregates for seeding analysis was conducted by centrifuging a reaction aliquot at 14 800 rpm in an Eppendorf centrifuge at 4 °C for 30 min, washing the pellet 2−3 times with PBS, resuspending in buffer, and determining the aggregate concentration by an HPLC analysis of a formic acid dissolved aliquot, as described.[26,28] SEC was on a Superdex 75 10/200 column (GE Health Sciences) equilibrated in PBS on an Agilent 1200 isocratic HPLC system with a flow rate of 0.4 mL/min and elution monitored at 214 nm. The column was calibrated with aprotinin, cytochrome C, ribonuclease, ovalbumin, and bovine serum albumin. In complex formation experiments, new peaks were characterized by analysis of 500 μL portions of the peak fractions on a reverse phase HPLC column with detection on an Agilent 1100 LC-MS system.

Electron Microscopy. Aliquots of aggregation reaction mixtures were taken at different time points and visualized by electron microscopy. A 3 μL sample was placed on a freshly glow-discharged carbon-coated grid, allowed to adsorb for 2 min, and washed with deionized water before staining with 2 μL of 1% uranyl acetate and blotting. Grids were imaged on a Tecnai T12 microscope (FEI Co., Hillsboro, OR) operating at 120 kV and 30000× magnification and equipped with an UltraScan 1000 CCD camera (Gatan, Pleasanton, CA) with postcolumn magnification of 1.4×.

Recombinant Protein Expression. The region encoding amino acids M1 to G115 of the αHtt-V_L 12.3 domain was amplified by PCR using plasmid DNA (pNES-VL12.3, a gift from Dane Wittrup) as template. The resulting amplicon was then inserted into a pET15b expression vector (Novagen), using NdeI and XhoI restriction sites at the 5′ and 3′ ends, respectively, generating an N-terminal His-tagged αHtt-V_L 12.3 domain construct. Following sequence verification, the V_L12.3−15b plasmid was transformed into *E. coli* Rosetta2 (DE3) cells (Novagen). Cultures were grown at 37 °C, induced with 1 mM IPTG at OD_{600} of ∼0.8, and further grown at 16 °C for 18 h for protein production. Cells were harvested by centrifugation, resuspended in TBS buffer (25 mM Tris.HCl, 150 mM NaCl, 3 mM NaN_3, and pH 8.0), and lyzed by sonication. Protein was purified by metal affinity chromatography on Ni^{2+}-derivatized HisTrap columns (GE Healthcare) using a linear (20−1000 mM) imidazole gradient for elution. Purified protein was digested with thrombin in TBS buffer for removal of the His tag (leaving a Gly-Ser-His sequence at the N-terminus of the V_L protein), followed by gel filtration on Superdex75 (GE Healthcare) in 20 mM sodium phosphate, 100 mM NaCl, and 3 mM NaN_3 (pH 6.0). Purified proteins were concentrated using centriprep concentrators (Millipore) up to ∼10 mg/mL, and the buffer was simultaneously exchanged to 20 mM sodium phosphate, 3 mM NaN_3, 90%/10% H_2O/D_2O (pH 6.0). The structure of the purified protein was confirmed by mass spectrometry.

RESULTS

A variety of proteolytic cleavage events generating short polyQ-containing fragments of htt have been implicated in the HD disease mechanism,[29] and the expression of expanded polyQ forms of such fragments, including one particular fragment, htt exon-1 (Figure 1), has been widely shown to lead to aggregation and/or toxicity in cells and animals.[30−35] Exon-1 consists of three well-defined sequence elements: the 17 amino acid htt^{NT} segment, the polyQ segment, and the Pro-rich

Peptide Name	Amino Acid Sequence
Htt exon 1	MATLEKLMKA FESLKSF--- QQQQQQQQQQ QQQQQQQQQQ QQQ------- ---------- PPPPPPPPPP-Htt_C[a]
htt^{NT}	MATLEKLMKA FESLKSF
$htt^{NT}Q_{30}P_6K_2$	MATLEKLMKA FESLKSF--- QQQQQQQQQQ QQQQQQQQQQ QQQQQQQQQQ ---------- PPPPPP---- KK
$htt^{NT}Q_{30}P_6K_2$ (F17W)	MATLEKLMKA FESLKSW--- QQQQQQQQQQ QQQQQQQQQQ QQQQQQQQQQ ---------- PPPPPP---- KK
$htt^{NT}Q_{37}P_{10}K_2$	MATLEKLMKA FESLKSF--- QQQQQQQQQQ QQQQQQQQQQ QQQQQQQQQQ QQQQQQQ--- PPPPPPPPPP KK
$Q_{37}P_{10}K_2$	QQQQQQQQQQ QQQQQQQQQQ QQQQQQQQQQ QQQQQQQ--- PPPPPPPPPP KK
MF-$Q_{37}P_{10}K_2$	M--------- ------F--- QQQQQQQQQQ QQQQQQQQQQ QQQQQQQQQQ QQQQQQQ--- PPPPPPPPPP KK
$K_2Q_{30}K_2$	KK QQQQQQQQQQ QQQQQQQQQQ QQQQQQQQQQ KK

[a]Htt_C = PQLPQPPPQA QPLLPQPQPP PPPPPPPPGP AVAEEPPLHR P

Figure 1. Sequences of the exon1 N-terminal fragment of huntingtin and the various synthetic peptides studied.

dx.doi.org/10.1021/bi3000929 | *Biochemistry* 2012, 51, 2706−2716

segment (Figure 1). Since chemically synthesized peptides containing the first two elements, plus polyPro segments as short as P_6, exhibit aggregation properties very similar to those of full length exon-1 [Sahoo, B., Singer, D., Zuchner, T., and Wetzel, R., manuscript in preparation], we have used such C-terminally truncated derivatives of htt exon1 to work out details of the aggregation mechanism.[16−18,36] Synthetic peptides studied in this paper are shown in Figure 1.

Compromising the htt^{NT} Role via Inhibition with htt^{NT} Peptides. Recently, we reported that peptides related to the htt^{NT} sequence can be effective, if transitory, inhibitors of the aggregation of polyQ-containing htt fragment peptides.[18] Thus, while 6 μM of htt$^{NT}Q_{30}P_6K_2$ exhibits measurable aggregation within several hours and is 50% aggregated by 18 h, the same concentration of peptide in the presence of a 1:1 ratio of htt^{NT} shows little aggregation after 18 h and requires ~80 h to reach 50% aggregation (Figure 2A). Since we reckoned that the polyQ element of htt$^{NT}Q_{30}P_6K_2$ might be capable of aggregating by several mechanisms, we inquired as to the nature of the residual aggregation that occurs in the presence of the htt^{NT} inhibitor. Electron micrographs of the noninhibited aggregation of htt$^{NT}Q_{30}P_6K_2$ show early formation of spherical oligomers (Figure 3B, 0.25 h), followed by protofibrils (Figure 3C, 2.5 h) and ultimately rough-edged fibrils (Figure 3D, 100 h).[16] In contrast, in addition to the expected[18] mixed oligomer inhibition complexes, early amyloid-like aggregates are observed at 5.5 h when htt$^{NT}Q_{30}P_6K_2$ is incubated in the presence of the htt^{NT} (Figure S1H), and larger aggregates observed at 8.0 h (Figure 3E and Figure S1I−P) exhibit the characteristic broad ribbons that are normally seen in amyloid aggregates of simple polyQ (Figure 3J); such aggregates are never observed in uninhibited reactions of htt$^{NT}Q_N$ peptides. EM images of the htt^{NT} inhibited reaction taken at subsequent times show aggregate morphologies more resembling the protofibrillar (Figure 3F, 45 h) and fibrillar (Figure 3G, 68 h) aggregates normally observed at earlier times in the non-inhibited aggregation of htt$^{NT}Q_{30}P_6K_2$ (Figure 3B,C). The progression of aggregate morphologies suggest that at early times in the htt^{NT} inhibited reaction there is a window within which htt$^{NT}Q_{30}P_6K_2$ peptides can nucleate amyloid growth via the pathway normally observed for simple polyQ peptides, leading to characteristic ribbon-like aggregates. Eventually, however, inhibition of htt^{NT}-mediated amyloid nucleation is overcome, and the characteristic aggregate morphologies observed in htt N-terminal peptide aggregation emerge.

Further kinetics studies add additional support to this view. An examination of the concentration dependence of the initial aggregation rates (Figure 4) of wild-type htt$^{NT}Q_{30}P_6K_2$ (■) and its F17W mutant (▲) in the absence of htt^{NT} inhibition yields log−log slopes of 1.20 and 0.95 as previously reported.[16] In contrast, the corresponding slope for the same peptide in the presence of inhibitor (△) is 2.65, which is very similar to the slope of 2.57 for aggregation of a simple $K_2Q_{30}K_2$ peptide (●) (Figure 4). This slope change is consistent with the EM data in suggesting that the early aggregation of htt$^{NT}Q_{30}P_6K_2$ in the presence of htt^{NT} occurs via the classical, nucleated growth mechanism previously determined for simple polyQ peptides.[14,15]

As a further test, the mature aggregates from the inhibited and noninhibited aggregation reactions of htt$^{NT}Q_{30}P_6K_2$, along with control amyloid-like aggregates of $K_2Q_{30}K_2$, were collected and studied for their seeding properties, as a measure of structural relatedness.[37,38] With htt$^{NT}Q_{30}P_6K_2$ monomers,

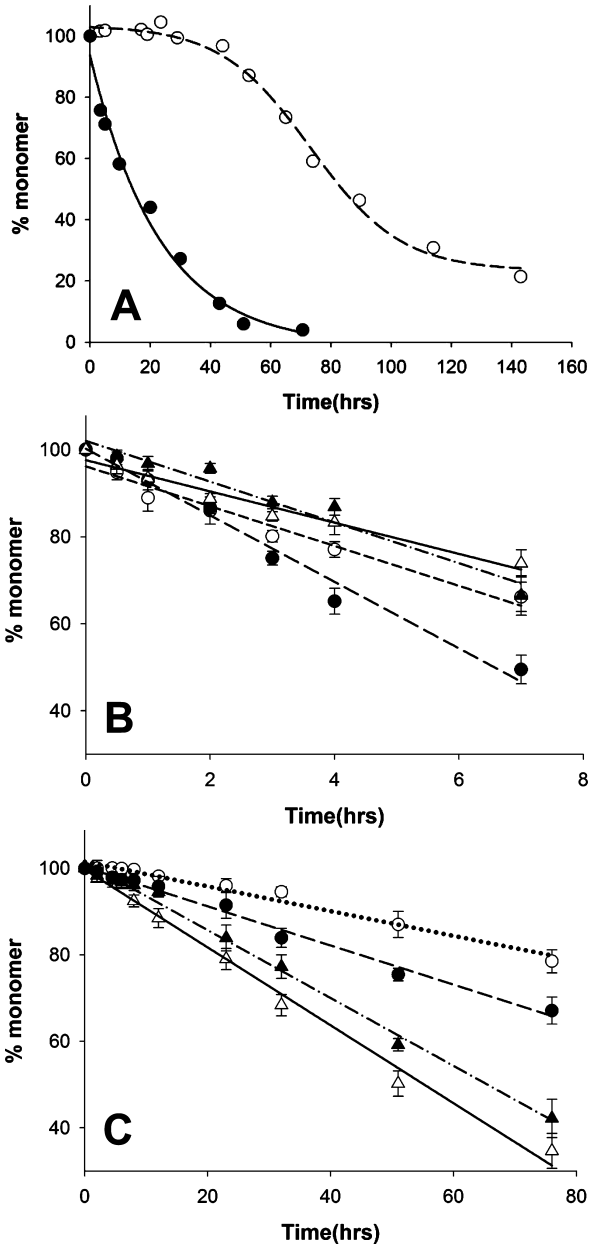

Figure 2. Aspects of htt^{NT} inhibition. (A) Kinetics of htt$^{NT}Q_{30}P_6K_2$ with (○) and without (●) htt^{NT} inhibition. (B) Aggregation of ~4 μM htt$^{NT}Q_{30}P_6K_2$ either with no addition (○) or seeded with 7.5 wt % of $K_2Q_{30}K_2$ fibrils (△); fibrils from htt$^{NT}Q_{30}P_6K_2$ aggregation with (▲) and without (●) added htt^{NT} inhibitor. (C) Aggregation of ~20 μM $K_2Q_{30}K_2$ either with no addition (○) or seeded with 5 wt % of $K_2Q_{30}K_2$ fibrils (△); fibrils from htt$^{NT}Q_{30}P_6K_2$ aggregation with (▲) and without (●) added htt^{NT} inhibitor. For comparison purposes, all data were fit to straight lines; linear fits are expected for efficient seeded elongation reactions,[37] but not for the spontaneous, unseeded reactions.[14−16] In fact, some deviation from linearity is seen in data from both of the nonseeded reactions.

only the product from the noninhibited aggregation of htt$^{NT}Q_{30}P_6K_2$ (●) exhibited significant enhancement compared with the nonseeded control (○), while $K_2Q_{30}K_2$ aggregates (△) and the products of htt^{NT}-inhibited htt$^{NT}Q_{30}P_6K_2$ aggregation (▲) were equally ineffective (Figure 2B). With $K_2Q_{30}K_2$ monomers, the product of htt^{NT}-inhibited aggregation of htt$^{NT}Q_{30}P_6K_2$ (▲) likewise behaved like simple $K_2Q_{30}K_2$ aggregates (△), with both aggregates

dx.doi.org/10.1021/bi3000929 | Biochemistry 2012, 51, 2706−2716

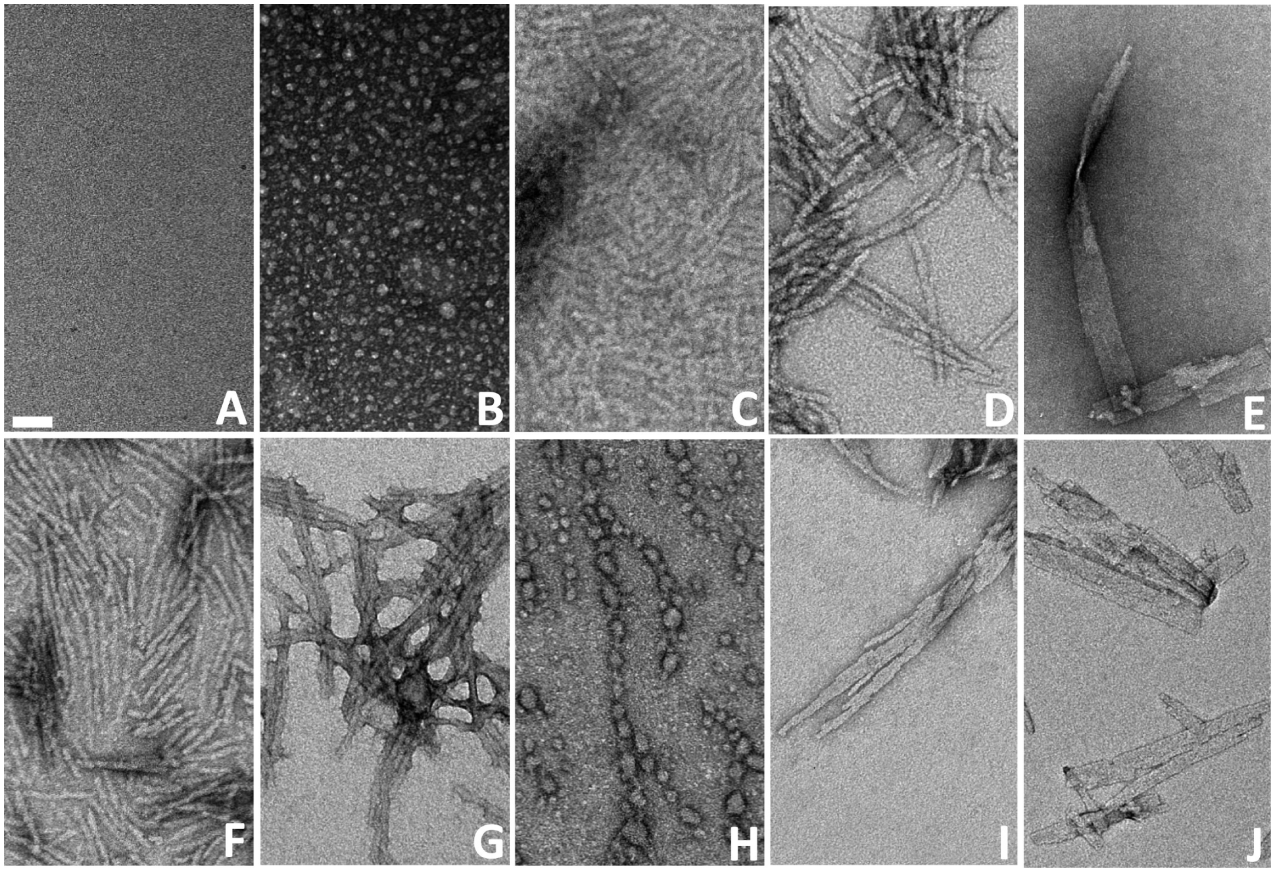

Figure 3. Electron micrographs of various polyglutamine aggregates. Empty grid (A); aggregation reaction of $htt^{NT}Q_{30}P_6K_2$ alone at 15 min (B), 2.5 h (C), and 100 h (D); aggregation of $htt^{NT}Q_{30}P_6K_2$ in the presence of a 1:1 molar ratio of htt^{NT} collected at 8 h (E), 45 h (F), and 68 h (G); aggregation of $htt^{NT}Q_{30}P_6K_2$ plus a 1:1 molar ratio of the antihtt^{NT} V_L protein collected at 120 h (H); aggregation of MF-$Q_{37}P_{10}K_2$, 74 h (I); final aggregates of $K_2Q_{30}K_2$ (J). The scale bar (A) of 50 nm is applicable to all panels.

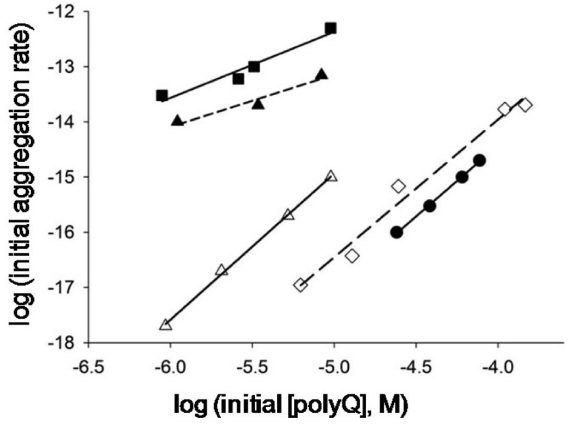

Figure 4. Concentration dependence of initial aggregation rates of polyQ peptides. Slopes of time-squared plots of initial aggregation kinetic data are plotted vs concentration in a log–log plot.[14] The slope of the log–log plot minus 2 is n^*, the critical nucleus.[14] Determination for $K_2Q_{30}K_2$ (●, slope = 2.57, n^* = 0.57), $htt^{NT}Q_{30}P_6$ (■, slope = 1.20, n^* = −0.80), $htt^{NT}Q_{30}P_6K_2$ (F17W) (▲, slope = 0.95, n^* = −1.05), $htt^{NT}Q_{30}P_6K_2$ (F17W) in the presence of htt^{NT} (△, slope = 2.65, n^* = 0.65), and MF-$Q_{37}P_{10}K_2$ (◇, slope = 2.57, n^* = 0.57). Previously, we found that the F17W mutation (Materials and Methods) has a negligible effect on aggregation kinetics.[16] Data for $K_2Q_{30}K_2$ and $htt^{NT}Q_{30}P_6K_2$ peptides alone are from ref 16.

significantly enhancing aggregation compared to the unseeded control (○) (Figure 2C). In contrast, the product of noninhibited $htt^{NT}Q_{30}P_6K_2$ aggregation (●) was an ineffective seed, producing no change from the unseeded rate (Figure 2C). Together the results show that (a) the seeding properties of noninhibited $htt^{NT}Q_{30}P_6K_2$ aggregation and $K_2Q_{30}K_2$ aggregation are different and (b) the seeding potential of the product of inhibited aggregation of $htt^{NT}Q_{30}P_6K_2$ is identical to that of $K_2Q_{30}K_2$ aggregates. These seeding results imply underlying structural similarities and differences. It is interesting that the final aggregates of the htt^{NT}-inhibited reaction behave like $K_2Q_{30}K_2$ aggregates, even though they are quite similar in appearance to the aggregates from the noninhibited $htt^{NT}Q_{30}P_6K_2$ reaction (Figure 3D,G). This shows that aggregate properties cannot always be correlated with EM morphologies.

Compromising the htt^{NT} Role via Inhibition with an antihtt^{NT} Intrabody. Previously, Wittrup and colleagues described a novel immunoglobulin-related molecule capable of binding the htt^{NT} segment of htt, obtained by a combination of mutagenesis and yeast surface display selection.[39] This light chain variable domain-related protein, αHtt-V_L 12.3, which lacks both a heavy chain partner and the normal, native Ig fold intradomain disulfide bond, exhibited a binding constant for htt^{NT} peptides in the low nanomolar range,[39,40] inhibited htt N-terminal fragment aggregation *in vitro*, and was a good inhibitor of htt aggregation and toxicity in mammalian cells in culture.[39] Interestingly, the X-ray crystal structure of a 1:1 complex of this VL 12.3 with an htt^{NT} fragment shows that htt^{NT} is bound in an α-helical conformation,[40] similar to the structure induced upon htt^{NT} self-assembly into tetramers and larger oligomers.[17,36]

dx.doi.org/10.1021/bi3000929 | *Biochemistry* 2012, 51, 2706–2716

We used a cDNA encoding this protein to engineer a vector for expression in *E. coli* (see Materials and Methods). After purification and proteolytic removal of the His tag, the 12 kDa protein was obtained and examined for its mechanism of aggregation inhibition.

In our standard sedimentation aggregation assay, this protein proved a very effective inhibitor of $htt^{NT}Q_{30}P_6K_2$ aggregation at a 1:1 molar ratio (Figure 5A). After a slow drop in soluble

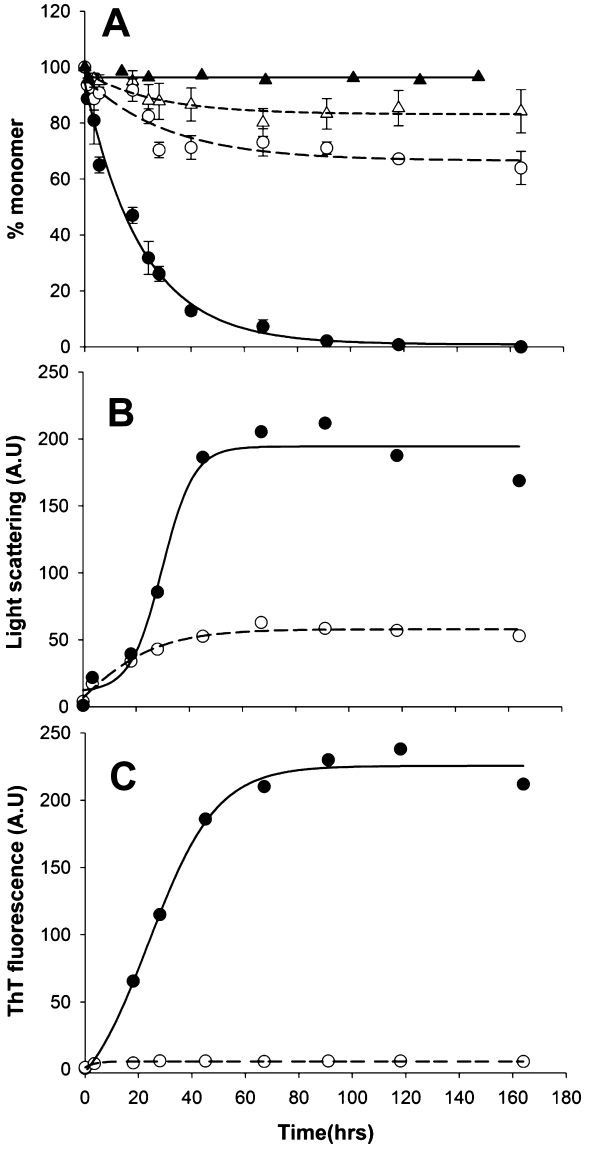

Figure 5. Kinetics of aggregation of a 1:1 molar ratio of V_L 12.3 and $htt^{NT}Q_{30}P_6K_2$ by the sedimentation (A), 90° light scattering (B), and ThT (C) assays. $Htt^{NT}Q_{30}P_6K_2$ with (○) and without (●) the V_L protein; V_L protein monomer concentration in mixture with $htt^{NT}Q_{30}P_6K_2$ (△); V_L protein incubated alone (▲).

$htt^{NT}Q_{30}P_6K_2$ in the inhibited reaction to about 70% the starting value, little or no further loss of monomer occurs up to over 150 h (Figure 5A, ○). A small but significant amount of the αHtt-V_L 12.3 domain protein also becomes pelletable over the same time frame (Figure 5A, △). In parallel with the generation of pelletable material, right angle light scattering confirmed the generation of protein particles (Figure 5B). At the same time, there is no detectible ThT signal throughout the incubation of $htt^{NT}Q_{30}P_6K_2$ with the αHtt-V_L 12.3 domain protein (Figure 5C), suggesting that the aggregates formed are not amyloid. Thus, in contrast to the inhibition by 1:1 ratios of htt^{NT} peptides, the αHtt-V_L 12.3 domain protein under the same conditions provides strong inhibition of htt^{NT}-mediated amyloid nucleation in polyQ-containing htt fragments. We conducted further experiments to explore this difference.

We first examined complex formation under native conditions between VL 12.3 and $htt^{NT}Q_{30}P_6K_2$ using SEC. As previously described,[40] we found that the αHtt-V_L 12.3 domain protein behaves aberrantly in SEC, late (Figure 6A, peak d), well after the position normally occupied by small solute molecules (Figure 6A,

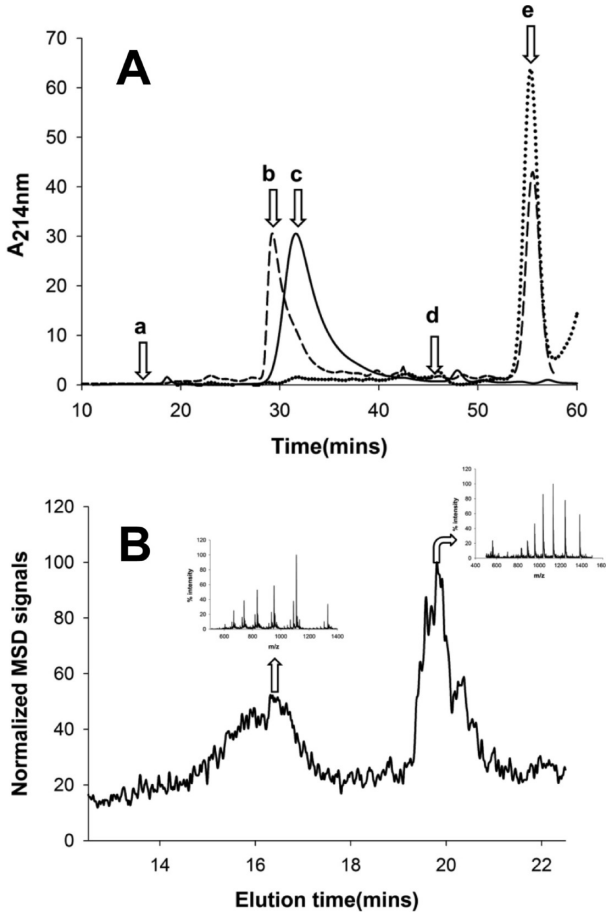

Figure 6. Size exclusion chromatography of the $antihtt^{NT}$ V_L 12.3 protein. (A) Chromatograms of $antihtt^{NT}$ V_L 12.3 protein alone (dotted line), $htt^{NT}Q_{30}P_6K_2$ alone (solid line), and a mixture of $htt^{NT}Q_{30}P_6K_2$ with excess $antihtt^{NT}$ V_L 12.3 protein (dashed line). Arrows indicate void volume (a), $htt^{NT}Q_{30}P_6K_2$: $antihtt^{NT}$ V_L 12.3 complex (b, 29.2 min, 12.6 kDa from standard curve; 19.0 kDa actual), $htt^{NT}Q_{30}P_6K_2$ alone (c, 31.6 min, 7.7 kDa from standard curve, 6.7 kDa actual), position of salt elution (d), $antihtt^{NT}$ V_L 12.3 protein alone (e); (B) LC-MS of the SEC peak b above identifying two components with the *m/z* of $htt^{NT}Q_{30}P_6K_2$ eluting at ~16.5 min and for the $antihtt^{NT}$ V_L 12.3 protein eluting at ~19.5 min.

peak d). In contrast, the $htt^{NT}Q_{30}P_6K_2$ peptide elutes at 31.6 min (Figure 6A, peak c), corresponding to a predicted MW of 7.7 kDa. The slight discrepancy between the SEC determined MW and the actual (6.7 kDa) is most likely due to the nonglobular nature of the htt N-terminal fragment (SEC standards used are all globular proteins; see Materials and Methods). A mixture of excess αHtt-V_L 12.3 domain protein with $htt^{NT}Q_{30}P_6K_2$ generates a new peak eluting at 29.2 min (Figure 6A, peak b), corresponding

dx.doi.org/10.1021/bi3000929 | *Biochemistry* 2012, 51, 2706–2716

to an SEC determined MW of 12.6 kDa. This is somewhat lower than expected (19.0 kDa) for a 1:1 complex, perhaps due to some residual interaction of the αHtt-V_L 12.3 domain component with the solid support. Interestingly, the SEC profile of the mixture also exhibits several higher MW forms, including a small peak corresponding to ~43 kDa (Figure 6A). The main 29.2 min SEC peak was collected and analyzed by LC-MS (see Materials and Methods). In the RP-HPLC of this SEC peak, two peaks were observed, giving MS signals corresponding to the known masses of $htt^{NT}Q_{30}P_6K_2$ and the αHtt-V_L 12.3 domain protein (Figure 6B). Thus, the major product of the initial interaction of $htt^{NT}Q_{30}P_6K_2$ and the αHtt-V_L 12.3 domain protein in solution is, as expected from other analyses,[40] a 1:1 complex.

Further examination of the incubated mixture of these two proteins by EM revealed additional higher assembly forms. EM images collected at 120 h consistently show a field of spherical aggregates with diameters in the 8−25 nm range (Figure 3H). There is a curious "beads-on-a-string" appearance to these images, the significance of which is not clear. These large oligomers presumably are the source of the ThT-negative (Figure 5C), light scattering positive (Figure 5B) material as well as the incomplete recovery of monomer in the sedimentation assay from solutions of $htt^{NT}Q_{30}P_6K_2$ and the αHtt-V_L 12.3 domain protein (Figure 5A). It is tempting to assign the observed strong inhibition of amyloid formation to the existence of these oligomers, in analogy to other peptide-based inhibitors of the aggregation of polyQ-containing htt fragments.[18] This interpretation does not hold up under scrutiny, however. Since oligomer formation does not nearly go to completion (Figure 5A), it would be expected that the residual (~70%) concentration of low-MW material should be capable of supporting the alternative amyloid formation pathway, as in the case of htt^{NT} inhibition described above. There is no evidence of this, however, by EM or other analysis. On the basis of the SEC analysis (Figure 6A), it is likely that the bulk of the $htt^{NT}Q_{30}P_6K_2$ in this solution is engaged in complex formation with the V_L 12.3 protein to generate a heterodimer (Figure 6A). It would therefore appear that this heterodimer formation is sufficient to very effectively block nucleation of polyQ amyloid formation. This suggests an ability of the 1:1 complex to interfere with the interactions of the polyQ chains that are required to engage the classical nucleated growth mechanism seen for simple polyQ peptides and for htt^{NT}-inhibited $htt^{NT}Q_{30}P_6K_2$ (see above). It is not clear how complexation of the V_L protein with the htt^{NT} segment alone might achieve this.

Compromising the htt^{NT} Role via Partial Excision. Previously, we showed that the polyQ-containing fragment of trypsin cleavage of $htt^{NT}Q_{37}P_{10}K_2$, namely, SF-$Q_{37}P_{10}K_2$, undergoes amyloid nucleation at a slower rate than the uncleaved molecule and exhibits a nucleation mechanism and aggregate morphologies identical to those from simple polyQ peptides.[15] To study the role of htt^{NT} domain function in the context of a full-length mutant htt in vivo, tg mouse experiments[41] have been initiated investigating the effect of expression of a full length htt molecule in which the 17 amino acid htt^{NT} sequence is replaced by the Met-Phe sequence [Yang, W., personal communication]. Here we investigate the impact of this sequence change in aggregation experiments *in vitro*.

As expected, the peptide MF-$Q_{37}P_{10}K_2$ (○) aggregates appreciably more slowly than a matched concentration of $htt^{NT}Q_{37}P_{10}K_2$ (●) (Figure 7A). At the same time, however, MF-$Q_{37}P_{10}K_2$ at a higher concentration (○) aggregates somewhat faster than the same concentration of $Q_{37}P_{10}K_2$ (●) (Figure 7B). Analysis of the concentration dependence of the initial aggregation of MF-$Q_{37}P_{10}K_2$ yields a log−log plot (Figure 4, ◇) slope of 2.5, almost identical to the slopes for $K_2Q_{30}K_2$ (●) and the htt^{NT}-inhibited aggregation of $htt^{NT}Q_{30}P_6K_2$ (△). Finally, the morphology of the MF-$Q_{37}P_{10}K_2$ aggregates (Figure 3I) is identical to typical amyloid-like aggregates of simple polyQ peptides (Figure 3J). Thus, aggregation kinetics and aggregate morphologies are consistent in indicating that this analogue of a trypsin-cleaved htt N-terminal fragment follows an aggregation pathway essentially identical to that of simple polyQ peptides.

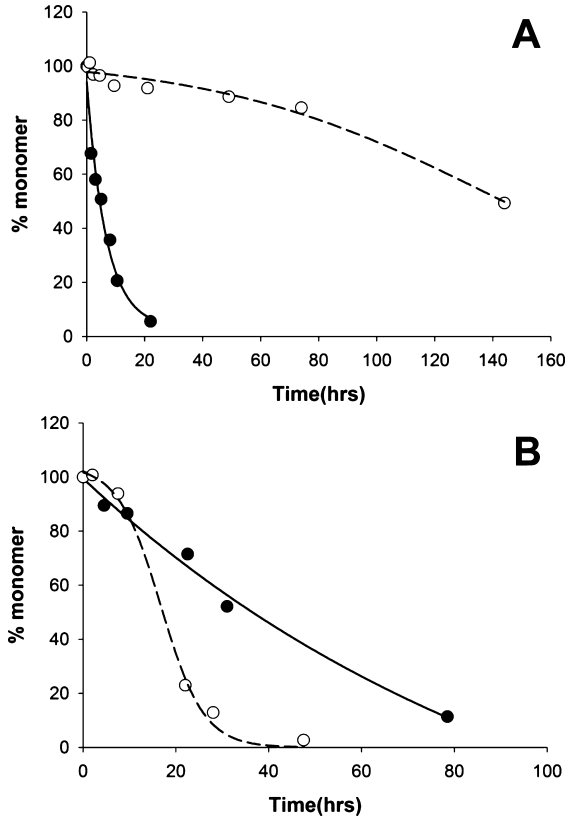

Figure 7. Kinetics of MF-$Q_{37}P_{10}K_2$ aggregation by the sedimentation assay: (A) aggregation of 6 μM MF-$Q_{37}P_{10}K_2$ (○) compared to 6 μM $htt^{NT}Q_{37}P_{10}K_2$ (●); (B) aggregation of 31 μM MF-$Q_{37}P_{10}K_2$ (○) compared to 48 μM $Q_{37}P_{10}K_2$ (●).

DISCUSSION

The phenomenon of aggregate polymorphism has emerged as a major area of interest in amyloid assembly and properties.[11,42,43] The ability to make multiple morphologies of stable products is nearly ubiquitous in amyloid systems and distinguishes them from native proteins. For example, not only do amyloidogenic peptides like Aβ exhibit a variety of aggregate nonamyloid morphologies, some of which may be particularly toxic,[44] but even mature amyloid fibrils of the same wild type Aβ peptide can exhibit a surprising number of distinct structural types.[45−47] The polymorphisms exhibited by mature amyloid fibrils are almost certainly linked to the phenomena of strain effects in prion biology, at least in yeast prion systems.[11,43] While the ability of protein aggregates to exhibit multiple, stable structural types is accounted for by the polymeric nature of protein assemblies,[48] the mechanistic basis for how growth conditions,[6,19,49−51] mutations,[7,52−54] and/or other, sporadic, factors[55]

dx.doi.org/10.1021/bi3000929 | *Biochemistry* 2012, 51, 2706−2716

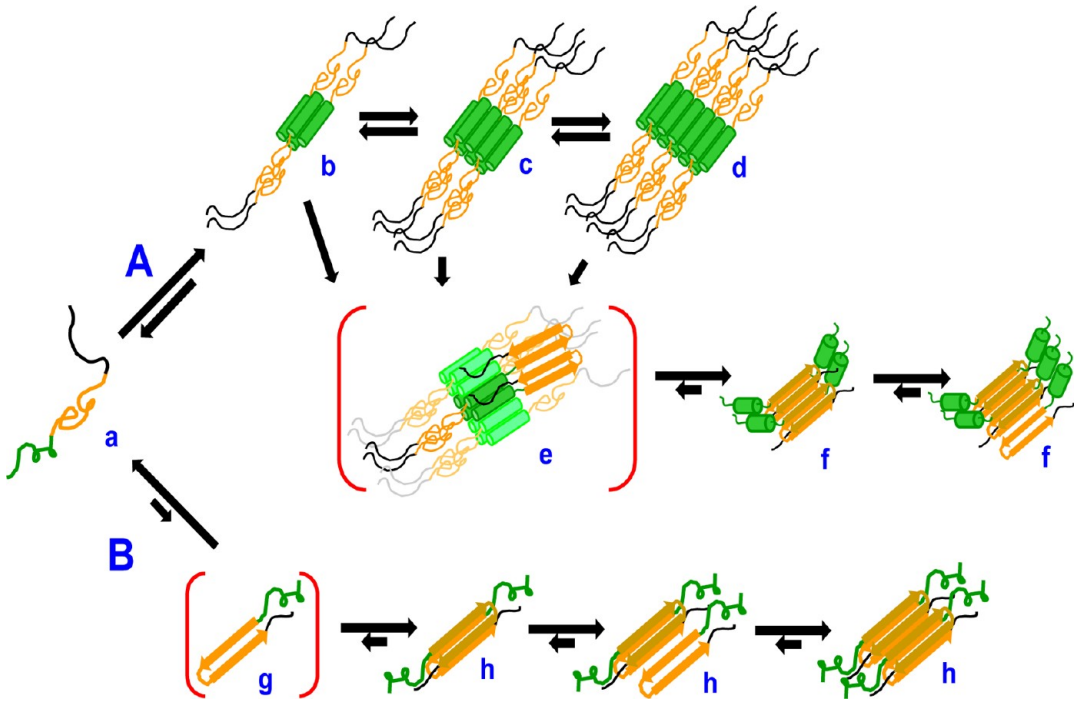

Figure 8. Kinetically competing pathways for nucleation of amyloid formation in polyQ-containing htt fragments. Monomeric fragment "a" (htt^{NT} = green, polyQ = orange, proline-rich = black) can enter both pathway A or pathway B to nucleate amyloid growth, with relative rates depending on structures and conditions. In pathway A, "a" can reversibly assemble into tetramer "b", which can further assemble into octomer "c", dodecamer "d", and higher order oligomers (not shown). These oligomers are held together primarily via α-helical packing of their htt^{NT} moieties while the polyQ and polyP segments are relatively solvent exposed with no defined structure. Each of "b", "c", and "d", as well as higher order oligomers, has a certain propensity to undergo amyloid nucleus ("e") formation in which some of the attached polyQ sequences assemble into amyloid. Once formed, nucleus "e" can initiate amyloid growth by monomer addition ("f"). In pathway B, "a" rarely and reversibly undergoes a highly energetically unfavorable folding event to generate a defined conformation or conformations ("g", the critical nucleus) capable of interacting with the polyQ of another htt fragment to initiate amyloid elongation ("h"). This is a schematic drawing meant to indicate general features of these pathways and structural details, such as the orientation of helices in the tetramer and the packing interfaces in higher oligomers, are yet to be worked out. Likewise, many structural features of the final aggregates of the B pathway and how they relate to the products of the A pathway have not been investigated.

control the kinetic accessibility that ultimately favors particular aggregate polymorphs has received less attention. This general problem may be particularly well-defined in the huntingtin system. While simple polyQ peptides are almost unique in the amyloid world in being able to assemble into amyloid fibrils without the mediation of nonamyloid intermediates,[15] certain flanking sequences to polyQ, such as the htt^{NT} segment of huntingtin,[16,17] mediate amyloid nucleation by undergoing an initial, independent assembly pathway.[2] At the same time, in contrast to the current wisdom that such oligomers tend to be the primary toxic agents in aggregation-based neurodegenerative diseases,[42] the situation may be different in polyQ diseases. We have argued that the reported low toxicity[24] of a htt exon1 analogue containing a particular type of proline-mutated polyQ segment[56] is evidence against a toxic role for nonamyloid oligomers of htt fragments.[18] Consistent with this view, a well-supported mechanism for aggregate toxicity in polyQ diseases, the recruitment/sequestration hypothesis,[22] is only likely to operate via mature amyloid-like polyQ aggregates, and not with oligomers, due to the relative abilities of these two aggregate classes to seed aggregate elongation[16] and hence recruit monomers. Perhaps related to such functional diversity, different morphologies of polyQ aggregates have been shown to exhibit different cytotoxicities.[19]

Our working model for the aggregation options open to polyQ-containing htt fragments is shown in Figure 8. Monomers (a) of such fragments are in principle capable of entering two distinct aggregation pathways. Pathway A involves the efficient formation of α-helix rich oligomers according to the pathway described previously.[16,17] In this pathway, the htt^{NT} segment of these peptides, which is disordered in the monomer state,[16] mediates α-helix bundle formation (b–d) that collects the disordered polyQ elements at a high local concentration and thereby facilitates the formation of polyQ amyloid nuclei (e) that can then elongate into β-rich amyloid like aggregates by monomer addition (f). (It should be noted that alternative models have also been described for how flanking sequences interact with polyQ sequences to effect aggregate formation.[57−59]) If, for any of a number of reasons, htt^{NT} mediated α-helix bundle formation is not feasible or efficient, polyQ-containing htt fragments can undergo the previously described[14,15] classical nucleation pathway. In this B pathway, for relatively long[15] polyQ peptides, the critical nucleus is a special, rare conformation of the monomer (g) that is capable of serving as the template for the initiation of amyloid elongation (h). This paper concerns cases in which the role of the htt^{NT} sequence is compromised by virtue of its removal or by the action of certain htt^{NT}-complexation agents. Elsewhere, we will describe what happens when htt^{NT} function is compromised due to sequence modifications within htt^{NT}, such as post-translational modifications[52] [Mishra, R., and Wetzel, R., manuscripts in preparation].

As previously described,[18] htt^{NT} and related sequences appear to inhibit pathway A by readily forming mixed α-helical oligomers with the polyQ-containing htt N-terminal fragment.

dx.doi.org/10.1021/bi3000929 | *Biochemistry* 2012, 51, 2706−2716

This dilutes the local concentration of the disordered polyQ segments and hence retards nucleation. At the same time, inhibition is incomplete, so that nucleation and growth of amyloid do finally occur.[18] As we shown here, when pathway A is transiently restricted, pathway B remains open, resulting in a concentration dependence characteristic of the B (and not the A) pathway and in the formation of polyQ amyloid aggregates that resemble aggregates of simple polyQ peptides both in the EM (Figure 3E and Figure S1I–P) and in their cross-seeding properties (Figure 2B,C). These data show that the lack of evidence for the simple polyQ aggregation pathway in $htt^{NT}Q_N$ peptides under most circumstances is not because this pathway is inactivated by the htt^{NT} moiety, but rather because it is outstripped kinetically by the alternate, htt^{NT}-mediated pathway. When the kinetic advantage of the htt^{NT}-mediated pathway is compromised, the simple polyQ nucleation and aggregation pathway effectively competes. The kinetic partitioning between these two well-characterized pathways of amyloid nucleation and growth provides a molecular basis for how certain chaperones can influence the course of huntingtin fragment aggregation.[57,60,61] In Figure 8, the products of pathway B are drawn to indicate the absence of the fully formed htt^{NT} α-helix that is known to exist in the final product of pathway A.[17,36] The fate of the htt^{NT} segment in these aggregates is unknown, however, and the altered structure is indicated schematically only as a reminder that the final aggregates must be structurally different at some level, since they are functionally different. In fact, the basis for the difference in seeding abilities of the final aggregates of the inhibited and noninhibited reactions is not clear. This may be a consequence of the amount of htt^{NT} inhibitor that appears to be bound to the fibrils.[18] Alternatively, it may reflect some very subtle structural difference of the polyQ β-sheet networks of these two fibrils.

Although the V_L 12.3 protein also likely inhibits pathway A by specifically complexing htt^{NT} and preventing its self-association, there is no evidence for the formation of pathway B products, in contrast to the results of htt^{NT} inhibition. Our data suggest that, even after long incubation, the bulk of a mixture of V_L 12.3 and htt N-terminal fragment consists of heterodimers of these two proteins, with only a minor portion of the proteins involved in the formation of large oligomers. It might have been expected that the polyQ segment of $htt^{NT}Q_{30}P_6K_2$ in these heterodimers might be as free to engage the B pathway (Figure 8) as are $htt^{NT}Q_{30}P_6K_2$ monomers under htt^{NT} inhibition, but there is no evidence that this pathway is open to the V_L 12.3/$htt^{NT}Q_N$ heterodimers. This implies that, in spite of the focus of V_L 12.3 on the htt^{NT} segment, the polyQ sequence in the heterodimer exists in a conformational state that resists the nucleation and/or elongation steps shown in the B pathway.

Since we previously showed that polyQ peptides containing a C-terminal polyPro extension undergo amyloid nucleation by the same mechanism as simple polyQ peptides,[62] it is not surprising that the peptide MF-$Q_{37}P_{10}K_2$ exhibits a log–log slope similar to that of $K_2Q_{30}K_2$ (Figure 4). The more rapid aggregation in the 40 μM range of MF-$Q_{37}P_{10}K_2$ compared with $Q_{37}P_{10}K_2$, however, shows that the MF sequence does play a role in aggregation. Just as the Ser-Phe sequence of htt^{NT} proximal to the polyQ has been shown to take part in β-sheet formation in the mature amyloid fibrils of htt N-terminal fragments,[36] it is possible that the polyQ proximal Met-Phe in MF-$Q_{37}P_{10}K_2$ is included in amyloid structure and by virtue of that might affect nucleation or elongation in a positive way. Regardless of this slight enhancing effect, however, it is also clear that MF-$Q_{37}P_{10}K_2$ aggregates much less rapidly than the corresponding $htt^{NT}Q_{37}P_{10}K_2$ (Figure 7A), and this rate difference is expected to be greatly enhanced at the low concentrations that obtain in the cell, based on a projection to low, cellular concentrations from their disparate concentration dependencies (Figure 4).

Although the htt^{NT} segment of htt has a number of important possible targeting and trafficking roles,[63−67] it is clear from these and other studies[16−18,36,52,57] that this flanking sequence of the polyQ also greatly contributes to biophysical properties. The data presented in this paper show that different fates of the htt^{NT} segment of polyQ-containing htt fragments can have different consequences, not only for aggregation rates but also for the mechanism of aggregation and hence for the structure and properties of the aggregate products. Thus, htt^{NT} inhibition of $htt^{NT}Q_N$ aggregation produces amyloid aggregates that are much more capable of recruiting other polyQ proteins into the growing aggregate than are the amyloid products of noninhibited aggregation reactions (Figure 2C). This observation is relevant to the recent description of the seeding ability of aggregates isolated from various HD tg mice[20] and to recruitment-sequestration models of polyQ toxicity.[21,22] It remains to be seen whether there exist molecules in the cell capable of producing htt^{NT}-like inhibitory effects, but certain molecular chaperones are attractive candidates for such molecules.[57,60,61] In contrast to htt^{NT}, the V_L 12.3 protein completely blocks amyloid formation *in vitro*, instead generating a mixture of heterodimers and nonamyloid oligomers. Given this result, the observation that this protein in cell culture inhibits both inclusion formation and cytotoxicity[68] is most consistent with the hypothesis, discussed above, that it is the amyloid fibril form of polyQ-containing htt fragments that are toxic, while nonamyloid oligomers are benign.[18] Given that the removal of the htt^{NT} segment from htt N-terminal fragments slows but does not abrogate polyQ amyloid formation, while completely eliminating the ability of such fragments to make nonamyloid oligomers, it will be interesting to consider the effects of this modification on disease course and neuronal pathology observed in ongoing tg mouse experiments [Gu et al., manuscript in preparation].

■ ASSOCIATED CONTENT

Supporting Information

A figure containing additional EM images of aggregates as well as a brief discussion of the provenance and significance of these aggregates. This material is available free of charge via the Internet at http://pubs.acs.org.

■ AUTHOR INFORMATION

Corresponding Author

*E-mail: rwetzel@pitt.edu; phone (412) 383-5271; fax (412) 648-9008.

Present Addresses

[§]Pharmaceutical Research and Development, Pfizer, Inc., Chesterfield, MO.

[⊥]Department of Biological Sciences and Bioengineering, Indian Institute of Technology, Kanpur, Uttar Pradesh, India.

Funding

Funding support was from the National Institutes of Health, R01 AG019322 (to R.W.), and from the Commonwealth of Pennsylvania, SAP #4100026429 (to A.M.G.).

Notes

The authors declare no competing financial interest.

■ ACKNOWLEDGMENTS

We gratefully acknowledge Dane Wittrup (MIT) for the gift of the cDNA encoding the αHtt-V_L 12.3 domain protein and discussions with William Yang (UCLA). We thank Bart Roland for providing some of the aggregation kinetics data and Drs. James Conway and Alexander Makhov for helpful discussions and access to the Structural Biology Department's cryo-EM facility.

■ ABBREVIATIONS

polyQ, polyglutamine; htt, huntingtin; htt^{NT}, 17 amino acid N-terminus of huntingtin preceding the polyQ sequence; $antihtt^{NT}$ V_L 12.3 protein, immunoglobulin light chain variable domain-derived htt^{NT} binding protein; HD, Huntington's disease.

■ REFERENCES

(1) Bates, G. P., and Benn, C. (2002) The polyglutamine diseases, in *Huntington's Disease* (Bates, G. P., Harper, P. S., and Jones, L., Eds.) pp 429−472, Oxford University Press, Oxford, UK.

(2) Wetzel, R. (2012) Physical chemistry of polyglutamine: Intriguing tales of a monotonous sequence. *J. Mol. Biol.*, DOI: 10.1016/j.jmb.2012.01.030.

(3) Scherzinger, E., Sittler, A., Schweiger, K., Heiser, V., Lurz, R., Hasenbank, R., Bates, G. P., Lehrach, H., and Wanker, E. E. (1999) Self-assembly of polyglutamine-containing huntingtin fragments into amyloid-like fibrils: implications for Huntington's disease pathology. *Proc. Natl. Acad. Sci. U. S. A. 96*, 4604−4609.

(4) Chen, S., Berthelier, V., Yang, W., and Wetzel, R. (2001) Polyglutamine aggregation behavior *in vitro* supports a recruitment mechanism of cytotoxicity. *J. Mol. Biol. 311*, 173−182.

(5) Wilburn, B., Rudnicki, D. D., Zhao, J., Weitz, T. M., Cheng, Y., Gu, X. F., Greiner, E., Park, C. S., Wang, N., Sopher, B. L., La Spada, A. R., Osmand, A., Margolis, R. L., Sun, Y. E., and Yang, X. W. (2011) An antisense CAG repeat transcript at JPH3 locus mediates expanded polyglutamine protein toxicity in Huntington's disease-like 2 mice. *Neuron 70*, 427−440.

(6) Wood, S. J., Maleeff, B., Hart, T., and Wetzel, R. (1996) Physical, morphological and functional differences between pH 5.8 and 7.4 aggregates of the Alzheimer's peptide Ab. *J. Mol. Biol. 256*, 870−877.

(7) Helms, L. R., and Wetzel, R. (1996) Specificity of abnormal assembly in immunoglobulin light chain deposition disease and amyloidosis. *J. Mol. Biol. 257*, 77−86.

(8) Kirkitadze, M. D., Bitan, G., and Teplow, D. B. (2002) Paradigm shifts in Alzheimer's disease and other neurodegenerative disorders: the emerging role of oligomeric assemblies. *J. Neurosci. Res. 69*, 567−577.

(9) Caughey, B., and Lansbury, P. T. (2003) Protofibrils, pores, fibrils, and neurodegeneration: separating the responsible protein aggregates from the innocent bystanders. *Annu. Rev. Neurosci. 26*, 267−298.

(10) Glabe, C. G., and Kayed, R. (2006) Common structure and toxic function of amyloid oligomers implies a common mechanism of pathogenesis. *Neurology 66*, S74−78.

(11) Kodali, R., and Wetzel, R. (2007) Polymorphism in the intermediates and products of amyloid assembly. *Curr. Opin. Struct. Biol. 17*, 48−57.

(12) Ross, C. A., and Poirier, M. A. (2005) Opinion: What is the role of protein aggregation in neurodegeneration? *Nat. Rev. Mol. Cell Biol. 6*, 891−898.

(13) Sathasivam, K., Lane, A., Legleiter, J., Warley, A., Woodman, B., Finkbeiner, S., Paganetti, P., Muchowski, P. J., Wilson, S., and Bates, G. P. (2010) Identical oligomeric and fibrillar structures captured from the brains of R6/2 and knock-in mouse models of Huntington's disease. *Hum. Mol. Genet. 19*, 65−78.

(14) Chen, S., Ferrone, F., and Wetzel, R. (2002) Huntington's Disease age-of-onset linked to polyglutamine aggregation nucleation. *Proc. Natl. Acad. Sci. U. S. A. 99*, 11884−11889.

(15) Kar, K., Jayaraman, M., Sahoo, B., Kodali, R., and Wetzel, R. (2011) Critical nucleus size for disease-related polyglutamine aggregation is repeat-length dependent. *Nat. Struct. Mol. Biol. 18*, 328−336.

(16) Thakur, A. K., Jayaraman, M., Mishra, R., Thakur, M., Chellgren, V. M., Byeon, I. J., Anjum, D. H., Kodali, R., Creamer, T. P., Conway, J. F., Gronenborn, A. M., and Wetzel, R. (2009) Polyglutamine disruption of the huntingtin exon 1 N terminus triggers a complex aggregation mechanism. *Nat. Struct. Mol. Biol. 16*, 380−389.

(17) Jayaraman, M., Kodali, R., Sahoo, B., Thakur, A. K., Mayasundari, A., Mishra, R., Peterson, C. B., and Wetzel, R. (2012) Slow amyloid nucleation via α-helix-rich oligomeric intermediates in short polyglutamine-containing Huntingtin fragments. *J. Mol. Biol. 415*, 881−899.

(18) Mishra, R., Jayaraman, M., Roland, B. P., Landrum, E., Fullam, R., Kodali, R., Thakur, A. K., Arduini, I., and Wetzel, R. (2012) Inhibiting nucleation of amyloid structure in a huntingtin fragment by targeting α-helix rich oligomeric intermediates. *J. Mol. Biol. 415*, 900−917.

(19) Nekooki-Machida, Y., Kurosawa, M., Nukina, N., Ito, K., Oda, T., and Tanaka, M. (2009) Distinct conformations of in vitro and in vivo amyloids of huntingtin-exon1 show different cytotoxicity. *Proc. Natl. Acad. Sci. U. S. A. 106*, 9679−9684.

(20) Gupta, S., Jie, S., and Colby, D. W. (2011) Protein misfolding detected early in the pathogenesis of a transgenic mouse model of Huntington's disease using an amyloid seeding assay. *J. Biol. Chem*, DOI: 10.1074/jbc.M111.305417.

(21) Nucifora, F. C. Jr., Sasaki, M., Peters, M. F., Huang, H., Cooper, J. K., Yamada, M., Takahashi, H., Tsuji, S., Troncoso, J., Dawson, V. L., Dawson, T. M., and Ross, C. A. (2001) Interference by huntingtin and atrophin-1 with cbp-mediated transcription leading to cellular toxicity. *Science 291*, 2423−2428.

(22) McCampbell, A., and Fischbeck, K. H. (2001) Polyglutamine and CBP: fatal attraction? *Nat. Med. 7*, 528−530.

(23) Bucciantini, M., Giannoni, E., Chiti, F., Baroni, F., Formigli, L., Zurdo, J., Taddei, N., Ramponi, G., Dobson, C. M., and Stefani, M. (2002) Inherent toxicity of aggregates implies a common mechanism for protein misfolding diseases. *Nature 416*, 507−511.

(24) Poirier, M. A., Jiang, H., and Ross, C. A. (2005) A structure-based analysis of huntingtin mutant polyglutamine aggregation and toxicity: evidence for a compact beta-sheet structure. *Hum. Mol. Genet. 14*, 765−774.

(25) Zhang, Q. C., Yeh, T. L., Leyva, A., Frank, L. G., Miller, J., Kim, Y. E., Langen, R., Finkbeiner, S., Amzel, M. L., Ross, C. A., and Poirier, M. A. (2011) A compact beta model of huntingtin toxicity. *J. Biol. Chem. 286*, 8188−8196.

(26) O'Nuallain, B., Thakur, A. K., Williams, A. D., Bhattacharyya, A. M., Chen, S., Thiagarajan, G., and Wetzel, R. (2006) Kinetics and thermodynamics of amyloid assembly using a high-performance liquid chromatography-based sedimentation assay. *Methods Enzymol. 413*, 34−74.

(27) Chen, S., Berthelier, V., Hamilton, J. B., O'Nuallain, B., and Wetzel, R. (2002) Amyloid-like features of polyglutamine aggregates and their assembly kinetics. *Biochemistry 41*, 7391−7399.

(28) Jayaraman, M., Thakur, A. K., Kar, K., Kodali, R., and Wetzel, R. (2011) Assays for studying nucleated aggregation of polyglutamine proteins. *Methods 53*, 246−254.

(29) Zuccato, C., Valenza, M., and Cattaneo, E. (2010) Molecular mechanisms and potential therapeutical targets in Huntington's disease. *Physiol. Rev. 90*, 905−981.

(30) Davies, S. W., Turmaine, M., Cozens, B. A., DiFiglia, M., Sharp, A. H., Ross, C. A., Scherzinger, E., Wanker, E. E., Mangiarini, L., and Bates, G. P. (1997) Formation of neuronal intranuclear inclusions underlies the neurological dysfunction in mice transgenic for the HD mutation. *Cell 90*, 537−548.

(31) Faber, P. W., Alter, J. R., MacDonald, M. E., and Hart, A. C. (1999) Polyglutamine-mediated dysfunction and apoptotic death of a Caenorhabditis elegans sensory neuron. *Proc. Natl. Acad. Sci. U. S. A. 96*, 179−184.
(32) Krobitsch, S., and Lindquist, S. (2000) Aggregation of huntingtin in yeast varies with the length of the polyglutamine expansion and the expression of chaperone proteins. *Proc. Natl. Acad. Sci. U. S. A. 97*, 1589−1594.
(33) Apostol, B. L., Kazantsev, A., Raffioni, S., Illes, K., Pallos, J., Bodai, L., Slepko, N., Bear, J. E., Gertler, F. B., Hersch, S., Housman, D. E., Marsh, J. L., and Thompson, L. M. (2003) A cell-based assay for aggregation inhibitors as therapeutics of polyglutamine-repeat disease and validation in Drosophila. *Proc. Natl. Acad. Sci. U. S. A. 100*, 5950−5955.
(34) Aiken, C. T., Tobin, A. J., and Schweitzer, E. S. (2004) A cell-based screen for drugs to treat Huntington's disease. *Neurobiol. Dis. 16*, 546−555.
(35) Wang, C. E., Tydlacka, S., Orr, A. L., Yang, S. H., Graham, R. K., Hayden, M. R., Li, S., Chan, A. W., and Li, X. J. (2008) Accumulation of N-terminal mutant huntingtin in mouse and monkey models implicated as a pathogenic mechanism in Huntington's disease. *Hum. Mol. Genet. 17*, 2738−2751.
(36) Sivanandam, V. N., Jayaraman, M., Hoop, C. L., Kodali, R., Wetzel, R., and van der Wel, P. C. (2011) The aggregation-enhancing huntingtin N-terminus is helical in amyloid fibrils. *J. Am. Chem. Soc. 133*, 4558−4566.
(37) O'Nuallain, B., Williams, A. D., Westermark, P., and Wetzel, R. (2004) Seeding specificity in amyloid growth induced by heterologous fibrils. *J. Biol. Chem. 279*, 17490−17499.
(38) Krebs, M. R., Morozova-Roche, L. A., Daniel, K., Robinson, C. V., and Dobson, C. M. (2004) Observation of sequence specificity in the seeding of protein amyloid fibrils. *Protein Sci. 13*, 1933−1938.
(39) Colby, D. W., Garg, P., Holden, T., Chao, G., Webster, J. M., Messer, A., Ingram, V. M., and Wittrup, K. D. (2004) Development of a human light chain variable domain (V(L)) intracellular antibody specific for the amino terminus of huntingtin via yeast surface display. *J. Mol. Biol. 342*, 901−912.
(40) Schiefner, A., Chatwell, L., Korner, J., Neumaier, I., Colby, D. W., Volkmer, R., Wittrup, K. D., and Skerra, A. (2011) A disulfide-free single-domain V(L) intrabody with blocking activity towards huntingtin reveals a novel mode of epitope recognition. *J. Mol. Biol. 414*, 337−355.
(41) Gray, M., Shirasaki, D. I., Cepeda, C., Andre, V. M., Wilburn, B., Lu, X.-H., Tao, J., Yamazaki, I., Li, S. -H., Sun, Y. -E., Li, X. -J., Levine, M. S., and Yang, X. W. (2008) Full-length human mutant huntingtin with a stable polyglutamine repeat can elicit progressive and selective neuropathogenesis in BACHD mice. *J. Neurosci., 28*, 6182−6195.
(42) Stefani, M. (2010) Structural polymorphism of amyloid oligomers and fibrils underlies different fibrillization pathways: immunogenicity and cytotoxicity. *Curr. Protein Pept. Sci. 11*, 343−354.
(43) Toyama, B. H., and Weissman, J. S. (2011) Amyloid structure: conformational diversity and consequences. *Annu. Rev. Biochem. 80*, 557−585.
(44) Glabe, C. G. (2008) Structural classification of toxic amyloid oligomers. *J. Biol. Chem. 283*, 29639−29643.
(45) Goldsbury, C. S., Wirtz, S., Muller, S. A., Sunderji, S., Wicki, P., Aebi, U., and Frey, P. (2000) Studies on the in vitro assembly of a beta 1−40: implications for the search for a beta fibril formation inhibitors. *J. Struct. Biol. 130*, 217−231.
(46) Paravastua, A. K., Leapman, R. D., Yau, W. M., and Tycko, R. (2008) Molecular structural basis for polymorphism in Alzheimer's beta-amyloid fibrils. *Proc. Natl. Acad. Sci. U. S. A. 105*, 18349−18354.
(47) Kodali, R., Williams, A. D., Chemuru, S., and Wetzel, R. (2010) A beta(1−40) forms five distinct amyloid structures whose beta-sheet contents and fibril stabilities are correlated. *J. Mol. Biol. 401*, 503−517.
(48) Wetzel, R., Shivaprasad, S., and Williams, A. D. (2007) Plasticity of amyloid fibrils. *Biochemistry 46*, 1−10.
(49) Tanaka, M., Chien, P., Naber, N., Cooke, R., and Weissman, J. S. (2004) Conformational variations in an infectious protein determine prion strain differences. *Nature 428*, 323−328.
(50) Kumar, S., and Udgaonkar, J. B. (2009) Conformational conversion may precede or follow aggregate elongation on alternative pathways of amyloid protofibril formation. *J. Mol. Biol. 385*, 1266−1276.
(51) Kumar, S., and Udgaonkar, J. B. (2009) Structurally distinct amyloid protofibrils form on separate pathways of aggregation of a small protein. *Biochemistry 48*, 6441−6449.
(52) Gu, X., Greiner, E. R., Mishra, R., Kodali, R., Osmand, A., Finkbeiner, S., Steffan, J. S., Thompson, L. M., Wetzel, R., and Yang, X. W. (2009) Serines 13 and 16 are critical determinants of full-length human mutant huntingtin induced disease pathogenesis in HD mice. *Neuron 64*, 828−840.
(53) Furukawa, Y., Kaneko, K., Yamanaka, K., and Nukina, N. (2010) Mutation-dependent polymorphism of Cu,Zn-superoxide dismutase aggregates in the familial form of amyotrophic lateral sclerosis. *J. Biol. Chem. 285*, 22221−22231.
(54) Ding, F., Furukawa, Y., Nukina, N., and Dokholyan, N. V. (2011) Local Unfolding of Cu, Zn Superoxide Dismutase Monomer Determines the Morphology of Fibrillar Aggregates. *J. Mol. Biol.*,
(55) Goldsbury, C., Frey, P., Olivieri, V., Aebi, U., and Muller, S. A. (2005) Multiple assembly pathways underlie amyloid-beta fibril polymorphisms. *J. Mol. Biol. 352*, 282−298.
(56) Thakur, A., and Wetzel, R. (2002) Mutational analysis of the structural organization of polyglutamine aggregates. *Proc. Natl. Acad. Sci. U. S. A. 99*, 17014−17019.
(57) Tam, S., Spiess, C., Auyeung, W., Joachimiak, L., Chen, B., Poirier, M. A., and Frydman, J. (2009) The chaperonin TRiC blocks a huntingtin sequence element that promotes the conformational switch to aggregation. *Nat. Struct. Mol. Biol. 16*, 1279−1285.
(58) Williamson, T. E., Vitalis, A., Crick, S. L., and Pappu, R. V. (2010) Modulation of polyglutamine conformations and dimer formation by the N-terminus of huntingtin. *J. Mol. Biol. 396*, 1295−1309.
(59) Fiumara, F., Fioriti, L., Kandel, E. R., and Hendrickson, W. A. (2010) Essential role of coiled coils for aggregation and activity of Q/N-rich prions and PolyQ proteins. *Cell 143*, 1121−1135.
(60) Wacker, J. L., Zareie, M. H., Fong, H., Sarikaya, M., and Muchowski, P. J. (2004) Hsp70 and Hsp40 attenuate formation of spherical and annular polyglutamine oligomers by partitioning monomer. *Nat. Struct. Mol. Biol. 11*, 1215−1222.
(61) Tam, S., Geller, R., Spiess, C., and Frydman, J. (2006) The chaperonin TRiC controls polyglutamine aggregation and toxicity through subunit-specific interactions. *Nat. Cell Biol. 8*, 1155−1162.
(62) Bhattacharyya, A., Thakur, A. K., Chellgren, V. M., Thiagarajan, G., Williams, A. D., Chellgren, B. W., Creamer, T. P., and Wetzel, R. (2006) Oligoproline effects on polyglutamine conformation and aggregation. *J. Mol. Biol. 355*, 524−535.
(63) Steffan, J. S., Agrawal, N., Pallos, J., Rockabrand, E., Trotman, L. C., Slepko, N., Illes, K., Lukacsovich, T., Zhu, Y. Z., Cattaneo, E., Pandolfi, P. P., Thompson, L. M., and Marsh, J. L. (2004) SUMO modification of Huntingtin and Huntington's disease pathology. *Science 304*, 100−104.
(64) Atwal, R. S., Xia, J., Pinchev, D., Taylor, J., Epand, R. M., and Truant, R. (2007) Huntingtin has a membrane association signal that can modulate huntingtin aggregation, nuclear entry and toxicity. *Hum. Mol. Genet. 16*, 2600−2615.
(65) Rockabrand, E., Slepko, N., Pantalone, A., Nukala, V. N., Kazantsev, A., Marsh, J. L., Sullivan, P. G., Steffan, J. S., Sensi, S. L., and Thompson, L. M. (2007) The first 17 amino acids of Huntingtin modulate its sub-cellular localization, aggregation and effects on calcium homeostasis. *Hum. Mol. Genet. 16*, 61−77.
(66) Thompson, L. M., Aiken, C. T., Kaltenbach, L. S., Agrawal, N., Illes, K., Khoshnan, A., Martinez-Vincente, M., Arrasate, M., JG, O. S.-R., Khashwji, H., Lukacsovich, T., Zhu, Y. Z., Lau, A. L., Massey, A., Hayden, M. R., Zeitlin, S. O., Finkbeiner, S., Green, K. N., Laferla, F. M., Bates, G., Huang, L., Patterson, P. H., Lo, D. C., Cuervo, A. M.,

Marsh, J. L., and Steffan, J. S. (2009) IKK phosphorylates Huntingtin and targets it for degradation by the proteasome and lysosome. *J. Cell Biol. 187*, 1083−1099.
(67) Atwal, R. S., Desmond, C. R., Caron, N., Maiuri, T., Xia, J. R., Sipione, S., and Truant, R. (2011) Kinase inhibitors modulate huntingtin cell localization and toxicity. *Nat. Chem. Biol. 7*, 453−460.
(68) Colby, D. W., Chu, Y., Cassady, J. P., Duennwald, M., Zazulak, H., Webster, J. M., Messer, A., Lindquist, S., Ingram, V. M., and Wittrup, K. D. (2004) Potent inhibition of huntingtin aggregation and cytotoxicity by a disulfide bond-free single-domain intracellular antibody. *Proc. Natl. Acad. Sci. U. S. A. 101*, 17616−17621.